A EUROPEAN JOURNAL

CHEMPHYSCHEM

OF CHEMICAL PHYSICS AND PHYSICAL CHEMISTRY

Accepted Article

Title: Formation, Structure and Composition of Methylaluminoxane

Authors: Mikko Linnolahti and Scott Collins

To be cited as: *ChemPhysChem* 10.1002/cphc.201700827

Link to VoR: http://dx.doi.org/10.1002/cphc.201700827

A Journal of

ChemPubSoc Europe

WILEY-VCH

www.chemphyschem.org

ARTICLE WILEY-VCH

Formation, Structure and Composition of Methylaluminoxane

Mikko Linnolahti,*[a] and Scott Collins [b]

Abstract: The structurally ill-characterized methylaluminoxane (MAO) is the activator of choice in olefin polymerization catalysis. We have carried out large scale and systematic quantum chemical calculations to simulate the thermodynamics of its formation by controlled hydrolysis of trimethylaluminum (TMA), extending the studies up to 25 Al atoms, and thus, for the first time, to the real size domain of MAO. In agreement with previous postulates on its structure, MAO is shown to favor cage-like structures, with common characteristics of containing associated TMA, regardless of size or shape. The sites containing associated TMA are reactive, and explain the function of MAO as a catalyst activator. The MAOs show overall composition in agreement with experiments, and make transition as a function of size from chains to rings to sheets to eventually cages, peaking at composition of $(MeAlO)_{16}(Me_3Al)_6$ having a tubular molecular structure and molecular weight of 1360 g mol^{-1}. The peak composition is in precise agreement with mass spectrometric studies of corresponding anions, which allow for both major and minor anions present to be detected.

Introduction

Methylaluminoxane (MAO) activator plays critical roles in catalytic preparation of polyolefins. Alongside with scavenging impurities, its reaction with a catalyst precursor, typically a group 4 metallocene or post-metallocene, yields the catalytically active species. The activation mechanism is not precisely known, but it involves a $[L_nMR]^+[MAO]^-$ ion pair as a key component.[1] The ion pair formation has been proposed to take place either by Lewis-acidic abstraction of an X^- leaving group from the metal pre-catalyst by the MAO, or by transfer of an $[Me_2Al]^+$ moiety from the MAO to the pre-catalyst.[2] Recent quantum chemical calculations using simplified metallocene/MAO model systems indicate that the both routes are viable.[3]

MAO has turned out to be a challenging substance for experimental structure characterization. In spite of decades of active research in both academy and industry, its structure remains elusive.[4] Structural characterization of MAO is of utmost importance for proper understanding of the function of the catalyst and for optimization of the activator. Various proposals for the possible structures have been made over the years. Early proposals included chains and rings involving three-coordinate Al and two-coordinate O.[5] However, computations,[6] alongside with experiments on closely related molecules,[7] have shown preference for four-coordinate Al and three-coordinate O. The preferred coordination numbers can be achieved for MAOs of a wide range of sizes by formation of cage-like or tubular structures.[8]

In place of educated guesses and chemical intuition, an alternative strategy for addressing the structure of MAO is to simulate its synthesis by controlled hydrolysis of trimethylaluminum (TMA).[9] Systematic studies on consecutive reactions involving MAOs, TMA, water and methane have been reported for up to octameric structures. The studies have consistently shown the formation of MAOs of general molecular formula of $(MeAlO)_n(Me_3Al)_m$ (where n = degree of oligomerization and m = number of associated TMA molecules and they have revealed structural transformation as a function of size from chains (n=1-2) to rings (n=3-4) to sheets (n=5-8).[3a,9d] From three to five TMAs (m=3-5) are associated into the $(MeAlO)_n$ core, in line with measured, average composition of $(Me_{1.4-1.5}AlO_{0.75-0.8})_n$.[10] The associated TMA forms sites with five-coordinate methyl groups bridging the adjacent aluminums, and which are likely the reactive sites of the MAO activator.

Detailed computations of the TMA hydrolysis reactions are very laborious due to a complex network of reactions involved, and have thus far not reached the size domain of ca. 20-30 Al atoms supported by experiments.[11] In this paper, as a result of several years of work and tens of thousands of calculations, we extended these studies to eventually reach the relevant size domain, which in parallel to mass spectrometric experiments allows us to make so far the most definitive conclusions regarding the structure of MAO.

Results and Discussion

Methodological considerations: *n*=1-8 revisited: As demonstrated previously,[9d] the thermodynamics of TMA hydrolysis can be described as a three-dimensional network of reactions involving MAOs and three elementary species: TMA, water and methane. The total reaction is $0.5(n+m)\ Me_6Al_2 + n\ H_2O \rightarrow (MeAlO)_n(Me_3Al)_m + 2n\ CH_4$, where n is the degree of oligomerization and m is the number of associated TMAs. The equation applies to all MAOs, which are in practice produced by considering the reactions with the elementary species to take place between every atom or bond and in all spatial orientations. For precise details, please see ref. [9d].

MAOs up to n = 8 have been previously produced by this procedure using MP2/TZVP level of theory.[3a] For reaching the size domain of MAOs supported by experiments, the choice of the method needs to be reconsidered, since the cost of and time for the MP2 calculations becomes unbearable with increasing

[a] Prof. M. Linnolahti
Department of Chemistry
University of Eastern Finland
Joensuu Campus, FI-80101 Joensuu, Finland
E-mail: mikko.linnolahti@uef.fi
[b] Dr. S. Collins, Visiting Scientist
Department of Chemistry
University of Victoria
3800 Finnerty Rd. Victoria, BC, Canada

Supporting information for this article is given via a link at the end of the document.

size of the molecules. Recent studies[8b,12] have suggested the M06-2X method[13] is a cost-effective replacement for the MP2 method in these systems, which we therefore evaluated for this purpose.

Table 1 lists the relative stabilities of the MAOs up to n=8 obtained by both MP2/TZVP and M06-2X/TZVP levels of theory. Overall, the stabilities are strikingly well reproduced by M06-2X; the discrepancy in energy values between the two methods averages 4.6 ± 2.0 kJ mol^{-1} over all compositions studied. Both methods show that 3–5 TMAs are associated into the $(MeAlO)_n$ core, and most importantly, the M06-2X method manages to reproduce the most stable composition for each degree of oligomerization. The success of the M06-2X method is due to its capability of reproducing the dispersive interactions of three-center, two-electron bonds involved in TMA[14] and in all MAOs containing associated TMA.

In addition, we note that for estimation of condensed phase entropies from gas phase calculations, multiplication of the $T\Delta S$ term by 2/3 is needed to correct for the solvation entropy.[15] The corrected relative stabilities are given in Table 1 (M06-2X-c). The effect of the correction seems minor, but it generally appears to slightly stabilize the MAOs having more associated TMAs. M06-2X-c is thus our method-of-choice for continuing towards the correct size domain of the MAOs.

Table 1. Relative stabilities[a] of the lowest energy isomers[b] of $(MeAlO)_n(Me_3Al)_m$, where n=1-8.

n	m	Formula	Mw (gmol^{-1})	MP2[b]	M06-2X	M06-2X-c[c]
1	0	$MeAlO$	58	380.6	374.7	397.0
1	1	Me_4Al_2O	130	104.0	109.4	130.6
1	2	Me_7Al_3O	202	28.3	25.1	35.4
1	3	$Me_{10}Al_4O$	274	19.7	11.4	3.6
2	0	$Me_2Al_2O_2$	116	181.5	187.7	201.6
2	1	$Me_5Al_3O_2$	188	107.8	108.2	123.3
2	2	$Me_8Al_4O_2$	260	23.2	20.2	29.0
2	3	$Me_{11}Al_5O_2$	332	16.6	11.8	13.7
2	4	$Me_{14}Al_6O_2$	404	13.2	8.2	2.6
3	0	$Me_3Al_3O_3$	174	113.6	114.6	127.3
3	1	$Me_6Al_4O_3$	246	73.0	67.5	74.5
3	2	$Me_9Al_5O_3$	318	34.7	33.3	40.1
3	3	$Me_{12}Al_6O_3$	390	8.2	4.6	6.6
4	0	$Me_4Al_4O_4$	232	75.0	69.9	77.7
4	1	$Me_7Al_5O_4$	304	53.6	47.4	53.5
4	2	$Me_{10}Al_6O_4$	376	28.6	24.3	28.1
4	3	$Me_{13}Al_7O_4$	448	3.4	0.9	2.9
4	**4**	**$Me_{16}Al_8O_4$**	**520**	**0.0**	**0.0**	**0.0**
5	0	$Me_5Al_5O_5$	290	70.3	66.7	35.0
5	1	$Me_8Al_6O_5$	362	28.4	21.6	27.5
5	2	$Me_{11}Al_7O_5$	434	19.7	13.1	17.2
5	3	$Me_{14}Al_8O_5$	506	5.8	3.1	6.4
5	4	$Me_{17}Al_9O_5$	578	0.6	–3.0	–3.3
6	0	$Me_6Al_6O_6$	348	39.4	35.4	41.6
6	1	$Me_9Al_7O_6$	420	23.4	18.6	23.5
6	2	$Me_{12}Al_8O_6$	492	18.0	12.4	15.6
6	3	$Me_{15}Al_9O_6$	564	14.2	5.5	6.0
6	4	$Me_{18}Al_{10}O_6$	636	0.0	–3.9	–3.5
7	0	$Me_7Al_7O_7$	406	42.9	39.2	45.5
7	1	$Me_{10}Al_8O_7$	478	16.6	10.7	15.6
7	2	$Me_{13}Al_9O_7$	550	10.9	4.7	7.7
7	3	$Me_{16}Al_{10}O_7$	622	7.3	2.0	4.0
7	4	$Me_{19}Al_{11}O_7$	694	2.6	–1.4	–0.3
8	0	$Me_8Al_8O_8$	464	22.6	18.8	24.4
8	1	$Me_{11}Al_9O_8$	536	16.0	10.5	15.1
8	2	$Me_{14}Al_{10}O_8$	608	7.0	0.5	3.5
8	3	$Me_{17}Al_{11}O_8$	680	8.3	1.3	2.6
8	4	$Me_{20}Al_{12}O_8$	752	3.6	0.4	1.1
8	5	$Me_{23}Al_{13}O_8$	825	1.8	–2.5	–3.1

[a] $\Delta(\Delta_r G)$ in kJmol$^{-1}n^{-1}$ for reaction $0.5(n+m)Me_6Al_2 + nH_2O \rightarrow (MeAlO)_n(Me_3Al)_m + 2nCH_4$ at T = 298K and p = 1atm. The values are given relative to n=4,m=4 (in bold). [b] From refs. [3a,9d] [c] After correction to condensed phase by multiplication of the $T\Delta S$ term by 2/3.

Extension to n = 9-18: The following figures illustrate the most stable MAOs that the procedure locates for each degree of oligomerization (Figure 1), and as a function of the number of aluminums (Figure 2). The structures are reported based on data up to n=18 and m=7, and thus up to 25 Al atoms, which is well within the size domain suggested by experiments.[11] The complete set containing the most stable MAOs for each combination of n and m is available in the Supporting Information.

We discuss the results as a function of degree of oligomerization, which is a more natural measure because of evolution of the MAOs from the TMA hydrolysis process. As reported previously, the structures undergo transformation from chains (n=1-2) to rings (n=3-4)[9d] to sheets with five-coordinate Al (n=5-7) to sheets with four-coordinate Al.[3a] Progressing towards the experimental size domain shows that the sheets become eventually transformed into cages at n=13, which confirms the long-standing consensus that MAO contains cage-like compounds.[4,5] The $(MeAlO)_n$ core of the cages is formed primarily of six-membered rings (to minimize ring strain) and entirely of four-coordinate Al and three-coordinate O. These three criteria can be satisfied only upon association of TMA onto the edges of the core. At edge environments, where Al four-coordination would be otherwise unattainable, three-coordination of O is sometimes compromised. In such edges, the Al four-coordination is obtained through formation of a four-coordinate O. The number of TMAs required to saturate all the edges is typically six, with the exception of the smallest MAOs.

The structural characteristics of the edge sites are independent of the sizes, forms and shapes of the MAOs. Figure 3 depicts the four ways by which associated Me_3Al saturates the edges. Bridging pentavalent carbon plays a key role in each case. Sites **A** and **B** possess latent Lewis-acidity through opening of the Al–C (bridging) bond upon ligand (anion) abstraction from the catalyst precursor. Sites **C** and **D** are prone to ionization through $[Me_2Al]^+$ cleavage, leaving an Me_3Al end group bound to a three-coordinate oxygen in the thereby formed $[MAO]^-$ anion.[2] These kind of sites are abundant in all MAOs, and are clearly responsible for its co-catalytic properties. It would be hence of high importance from the point of view of rational catalyst development to be able to control the structures of the MAOs and thus the properties of the reactive sites.

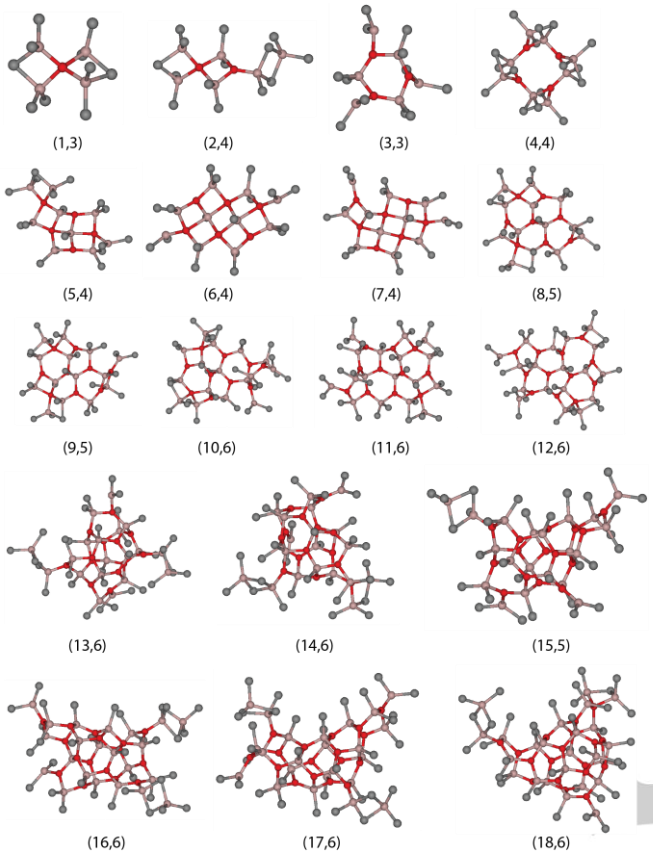

Figure 1. The most stable MAOs located for each degree of oligomerization. Nomenclature: (*n*,*m*) for MAOs of general formula $(MeAlO)_n(Me_3Al)_m$. Hydrogens are omitted for clarity with CH_3 groups in grey, Al atoms in pink and O atoms in red.

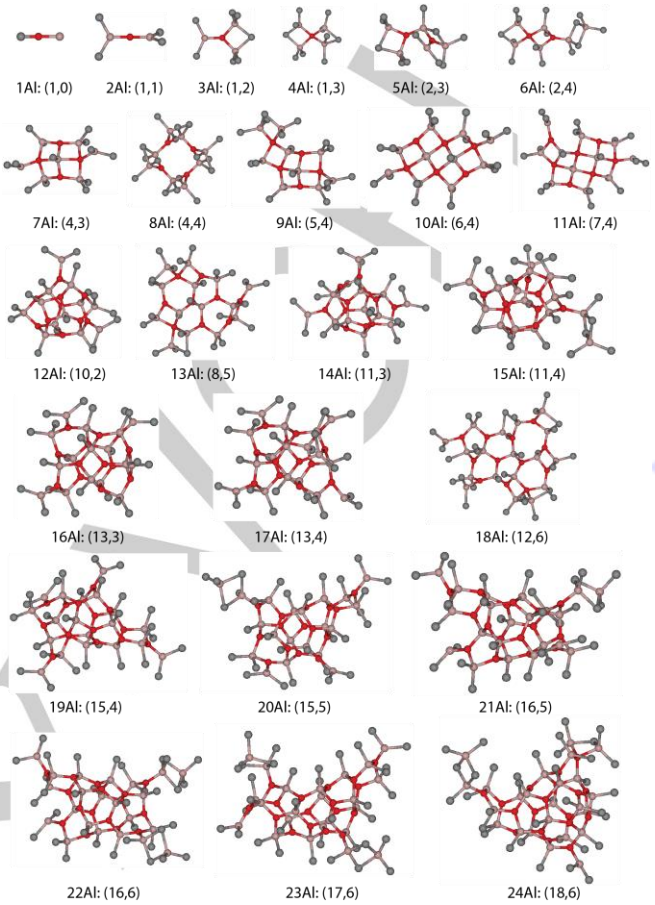

Figure 2. The most stable MAOs located for each number of aluminums. Nomenclature: (*n*,*m*) for MAOs of general formula $(MeAlO)_n(Me_3Al)_m$. Hydrogens are omitted for clarity.

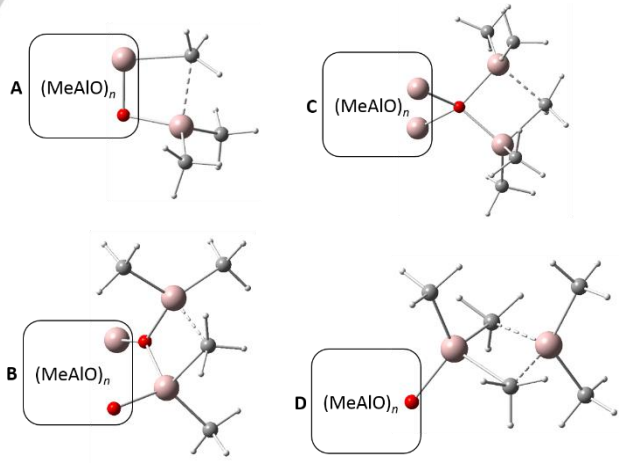

Figure 3. Association of Me_3Al onto the edges of MAOs to form reactive sites. The squares depict the $(MeAlO)_n$ cores of the MAOs.

The relative stabilities of the MAOs are given in Table 2, with n=4,m=4 as a reference to maintain comparability with Table 1. Figure 4 shows the relative stabilities as a function of both degree of oligomerization and the number of Al atoms using the most stable composition as a reference. The same pattern emerges from the two x-axes, with a shift of six units, which reflects the tendency of the MAOs to bind overall six TMAs for full saturation of the edges. The stabilities improve, though not monotonously, from chains to rings to sheets to cages, eventually bottoming at n=16 for the data set. Having six associated TMAs, the minimum has 22 Al atoms and a molecular formula of $(MeAlO)_{16}(Me_3Al)_6$. It has an elongated structure and it possesses reactive sites of type **A** and **D** (see Figure 3), and thus holds potential for pre-catalyst activation by both Lewis-acidic abstraction and $[Me_2Al]^+$ cleavage. We have previously employed this MAO model for studying the mechanisms for ion-pair formation,[16] so the present work provides a complete justification for its use as a model system.

Table 2. Relative stabilities[a] of the lowest energy isomers of $(MeAlO)_n(Me_3Al)_m$, where n=9-18, calculated by the M06-2X-c method.

n	m	Formula	Mw (gmol^{-1})	$\Delta(\Delta_rG)$
9	0	$Me_9Al_9O_9$	522	17.9
9	1	$Me_{12}Al_{10}O_9$	594	10.9
9	2	$Me_{15}Al_{11}O_9$	666	2.5
9	3	$Me_{18}Al_{12}O_9$	738	0.5
9	4	$Me_{21}Al_{13}O_9$	811	–1.0
9	5	$Me_{24}Al_{14}O_9$	883	–2.4
10	0	$Me_{10}Al_{10}O_{10}$	580	17.3
10	1	$Me_{13}Al_{11}O_{10}$	652	6.1
10	2	$Me_{16}Al_{12}O_{10}$	724	–1.1
10	3	$Me_{19}Al_{13}O_{10}$	796	–1.2
10	4	$Me_{22}Al_{14}O_{10}$	869	0.1
10	5	$Me_{25}Al_{15}O_{10}$	941	–0.1
10	6	$Me_{28}Al_{16}O_{10}$	1013	–1.3
11	0	$Me_{11}Al_{11}O_{11}$	638	11.5
11	1	$Me_{14}Al_{12}O_{11}$	710	4.0
11	2	$Me_{17}Al_{13}O_{11}$	782	–1.5
11	3	$Me_{20}Al_{14}O_{11}$	854	–2.9
11	4	$Me_{23}Al_{15}O_{11}$	927	–4.1
11	5	$Me_{26}Al_{16}O_{11}$	999	–2.7
11	6	$Me_{29}Al_{17}O_{11}$	1071	–4.1
12	0	$Me_{12}Al_{12}O_{12}$	696	5.8
12	1	$Me_{15}Al_{13}O_{12}$	768	4.9
12	2	$Me_{18}Al_{14}O_{12}$	840	–1.6
12	3	$Me_{21}Al_{15}O_{12}$	912	–2.6
12	4	$Me_{24}Al_{16}O_{12}$	985	–2.8
12	5	$Me_{27}Al_{17}O_{12}$	1057	–3.9
12	6	$Me_{30}Al_{18}O_{12}$	1129	–5.4
13	0	$Me_{13}Al_{13}O_{13}$	754	11.1
13	1	$Me_{16}Al_{14}O_{13}$	826	2.5
13	2	$Me_{19}Al_{15}O_{13}$	898	0.4
13	3	$Me_{22}Al_{16}O_{13}$	971	–3.0
13	4	$Me_{25}Al_{17}O_{13}$	1043	–4.7
13	5	$Me_{28}Al_{18}O_{13}$	1115	–4.8
13	6	$Me_{31}Al_{19}O_{13}$	1187	–5.4
13	7	$Me_{34}Al_{20}O_{13}$	1259	–3.5
14	0	$Me_{14}Al_{14}O_{14}$	812	4.4
14	1	$Me_{17}Al_{15}O_{14}$	884	–0.7
14	2	$Me_{20}Al_{16}O_{14}$	956	–2.2
14	3	$Me_{23}Al_{17}O_{14}$	1029	–3.7
14	4	$Me_{26}Al_{18}O_{14}$	1101	–4.8
14	5	$Me_{29}Al_{19}O_{14}$	1173	–5.4
14	6	$Me_{32}Al_{20}O_{14}$	1245	–6.1
14	7	$Me_{35}Al_{21}O_{14}$	1317	–6.0
15	0	$Me_{15}Al_{15}O_{15}$	870	0.8
15	1	$Me_{18}Al_{16}O_{15}$	942	–1.5
15	2	$Me_{21}Al_{17}O_{15}$	1014	–3.4
15	3	$Me_{24}Al_{18}O_{15}$	1087	–3.8
15	4	$Me_{27}Al_{19}O_{15}$	1159	–5.7
15	5	$Me_{30}Al_{20}O_{15}$	1231	–6.2
15	6	$Me_{33}Al_{21}O_{15}$	1303	–5.4
15	7	$Me_{36}Al_{22}O_{15}$	1375	–4.7
16	0	$Me_{16}Al_{16}O_{16}$	928	0.1
16	1	$Me_{19}Al_{17}O_{16}$	1000	–1.4
16	2	$Me_{22}Al_{18}O_{16}$	1072	–4.9
16	3	$Me_{25}Al_{19}O_{16}$	1145	–5.4
16	4	$Me_{28}Al_{20}O_{16}$	1217	–5.5
16	5	$Me_{31}Al_{21}O_{16}$	1289	–7.4
16	6	$Me_{34}Al_{22}O_{16}$	1361	–7.5
16	7	$Me_{37}Al_{23}O_{16}$	1433	–3.7
17	0	$Me_{17}Al_{17}O_{17}$	986	4.0
17	1	$Me_{20}Al_{18}O_{17}$	1058	–1.9
17	2	$Me_{23}Al_{19}O_{17}$	1131	–4.5
17	3	$Me_{26}Al_{20}O_{17}$	1203	–4.6
17	4	$Me_{29}Al_{21}O_{17}$	1275	–6.4
17	5	$Me_{32}Al_{22}O_{17}$	1347	–6.5
17	6	$Me_{35}Al_{23}O_{17}$	1419	–6.8
17	7	$Me_{38}Al_{24}O_{17}$	1491	–3.9
18	0	$Me_{18}Al_{18}O_{18}$	1044	3.5
18	1	$Me_{21}Al_{19}O_{18}$	1116	–2.2
18	2	$Me_{24}Al_{20}O_{18}$	1189	–4.2
18	3	$Me_{27}Al_{21}O_{18}$	1261	–5.3
18	4	$Me_{30}Al_{22}O_{18}$	1333	–6.1
18	5	$Me_{33}Al_{23}O_{18}$	1405	–5.9
18	6	$Me_{36}Al_{24}O_{18}$	1477	–6.5
18	7	$Me_{39}Al_{25}O_{18}$	1549	–4.4

[a] $\Delta(\Delta_rG)$ in kJmol$^{-1}n^{-1}$ for reaction $0.5(n+m)Me_6Al_2 + nH_2O \rightarrow (MeAlO)_n(Me_3Al)_m + 2nCH_4$ at T = 298K and p = 1atm. The values are given relative to n=4,m=4.

Another way to present the size dependency of the relative stability, allowing to include all combinations of n and m in the same graph, is to plot the relative stabilities as a function of molecular weight (Figure 5A). From the Boltzmann distribution, one can then convert the relative stabilities to relative abundances (Figure 5B). The results suggest a peak composition at n=16,m=6 in TMA association/dissociation equilibrium with n=16,m=5. Lower amounts of n=17,m=6 and n=18,m=6 are present. Calculations for the MAO mixture in Figure 5B give an average molecular weight of 1163 g mol^{-1} and an average composition of $(Me_{1.48}AlO_{0.76})_n$.

Experimental composition of MAO mixtures: MAO has resisted fractionation into its individual components and thus there is still no precise information on the mass distribution of neutral components.[17] However, recently, the ESI MS of MAO and various additives that lead to ion-pair formation has been studied in negative ionization mode in fluorobenzene solution.[2b,16] In this case it is the anion distribution derived from MAO that is being studied.

Relative stabilities for the anions $[(MeAlO)_n(Me_3Al)_mMe]^-$ detected in MAO that has been treated with equimolar octamethyltrisiloxane (OMTS) to form $[Me_2Al(OMTS][(MeAlO)_n(Me_3Al)_mMe]$ ion pairs[16b] are depicted in Figure 6. Over the size domain of interest (i.e. $7 \le n \le 18$) one can detect a series of anions with varying degrees of polymerization (n) and different amounts of associated TMA (m). Also shown in this Figure are the relative stabilities of plausible neutral precursors for these anions.

Since the anions could form by either methide or Me_2Al^+ abstraction, there are (at least) two possible precursors for each observed anion. The distribution of the neutrals vs. the anions cannot be directly compared, because the intensity of ions detected by ESI MS depends on factors in addition to solution concentration, the most important being the surface activity of

the ion in question. However, the anion distribution is consistent with the calculations, which show that higher MW aluminoxanes are more stable and thus available for reaction with suitable additives.

Some lower MW anions appear over- (or under-) represented in this mixture compared with the stability of possible precursors. The most striking example is the anion with *n*=10,*m*=4; both neutral precursors with *n*=10,*m*=4 or *m*=5 have *nido*-(sheet) like structures (e.g. Figure 1, *n*=10,*m*=6) and perhaps a structural change occurs on forming the same anion from either. In other cases, the two precursors differ significantly in structure – e.g. *n*=12,*m*=5 is closo- (cage-like) while *n*=12,*m*=6 is sheet-like (Figure 1) and though both precursors are of similar stability, one may be more reactive to anion formation than the other. Future work will focus on these important aspects of MAO structure and function.

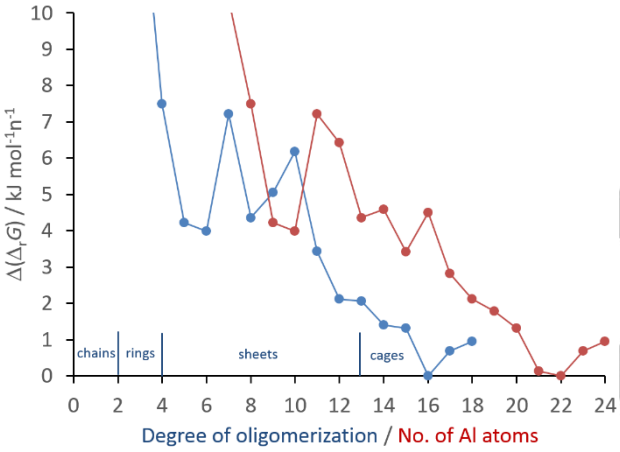

Figure 4. Relative stabilities (T = 298K and p = 1atm) of the MAOs as a function of degree of oligomerization, n (blue) and the number of Al atoms (red). The molecular structures are illustrated in Figures 1 and 2, respectively.

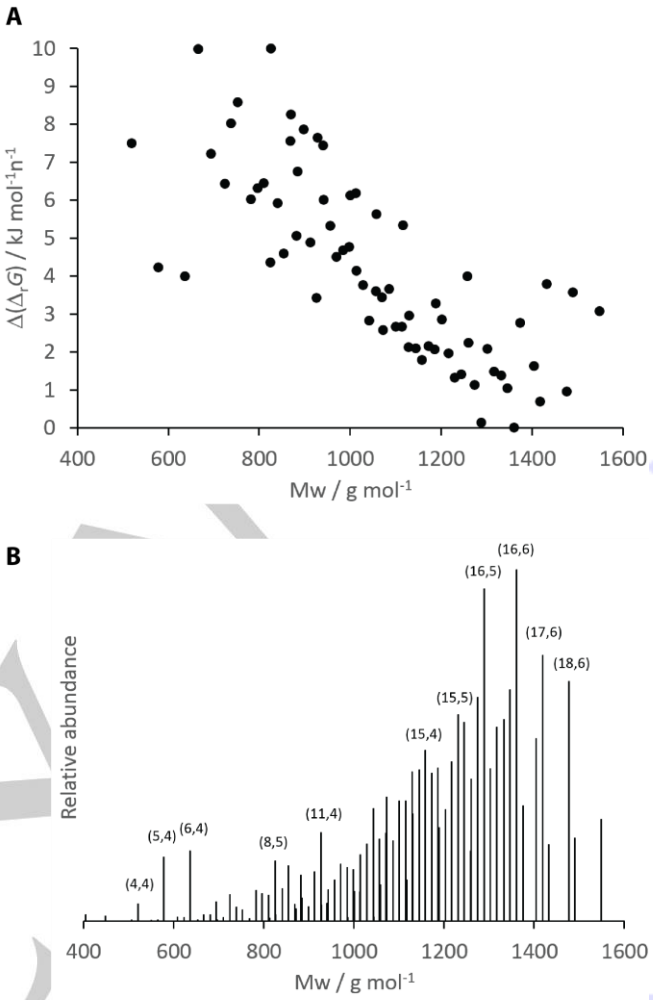

Figure 5. Relative stabilities (A) and abundancies (B) of the MAOs as a function of molecular weight.

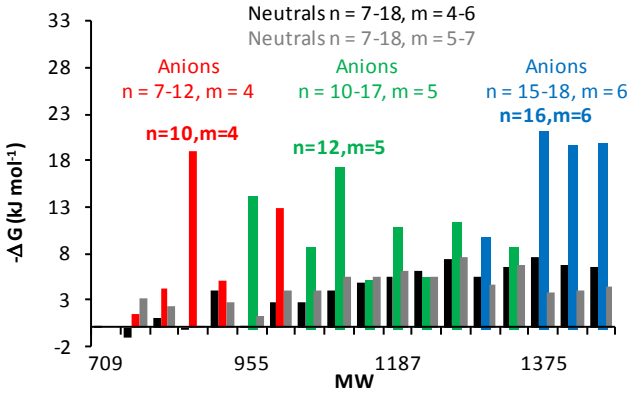

Figure 6. Relative stability of anions (in color) detected by ESI MS compared with neutral precursors (gray scale).The anion stabilities are expressed with reference to *n*=7,*m*=4, the least abundant anion with *m*/*z* = 709, while those for the neutrals are relative to *n*=4,*m*=4 (Table 2). The anions highlighted in bold in each *n*,*m* series have been characterized by MS-MS experiments [16b].

Conclusions

The formation of MAOs of formula $(MeAlO)_n(Me_3Al)_m$ has been studied computationally up to the real size domain of MAO by following in detail the TMA hydrolysis reactions up to n=18 and m=7. All MAOs, independent of size and shape, contain associated TMAs, which stabilize the edges and introduce bridging pentavalent methyl groups into the MAOs. Typically, six TMAs are required to saturate the edges, which thereby form the sites of cocatalytic activity in olefin polymerization.

The MAOs show transition from chains to rings to sheets to cage-like structures as a function of size, the relative stabilities improving in the same order. Approaching the real size domain of the MAOs, cages thus eventually become favored over the other structural alternatives. Transition to cages takes place at n=13, and the stabilities peak at n=16,m=6 for the data set, showing preference for a tubular molecular structure. The results are in a remarkable agreement with mass spectrometric studies on the corresponding anions and with the measured average composition of the MAO. The long sought main structural features of the MAO thus appear revealed, which paves way for detailed understanding of the catalyst activation process in future studies.

Experimental Section

Computational details: The MAOs were produced by systematically following the three-dimensional network of reactions involving the MAOs, TMA, water and methane, as described in ref. [9d], using the BOTTOM approach described in ref. [3a]. As recommended for systems containing dispersive interactions due to bridging methyl groups,[12] M06-2X functional[13] was used in combination with def-TZVP basis set.[18] Vibrational frequencies were calculated by the harmonic approximation for the lowest energy isomer of each composition to verify them as a minimum and to obtain Gibbs energies at T = 298 K and p = 1 atm. The Gibbs energies obtained from the gas phase calculations were corrected by multiplication of the $T\Delta S$ term by 2/3 for estimation of condensed phase entropies.[15] All calculations were carried out by Gaussian 09.[19]

ESI-MS analysis details: Processing of a total ion chromatogram (TIC) of an equimolar mixture of MAO and OMTS in fluorobenzene [16b] using the MassLynx software provided a negative ion mass spectrum over the m/z range 50-3000 Da; anions are detected from n=7 to n=30 (m/z 2403, m=9) for this particular sample. Individual anion peaks (including isotopomers) were integrated between n=7-18 to provide intensity data that was normalized to (divided through by) the TIC within MS Excel. These normalized intensity data showed minor fluctuations in intensity with time, reflecting variations in both individual ion intensity as well as the TIC, which is characteristic of MAO solutions. For those regions where the normalized intensity data was stable, average intensity values were determined. These were used to create the column chart in Figure 6.

Acknowledgements

ML acknowledges grants from the 7th Framework Programme of the European Commission (246274), from the Academy of Finland (251448), and of computer capacity from the Finnish Grid and Cloud Infrastructure (urn:nbn:fi:research-infras-2016072533). SC acknowledges the University of Victoria for a Visiting Scientist appointment. Harmen S. Zijlstra of the University of Victoria is thanked for sharing ESI MS data with us from ref. [16b].

Keywords: ab initio calculations • polymerization • homogeneous catalysis • structure elucidation • cage compounds

[1] a) M. Bochmann, *Organometallics* **2010**, *29*, 4711. b) E. Y. Chen, T. J. Marks, *Chem. Rev.* **2000**, *100*, 1391.

[2] a) L. Luo, S. A. Sangokoya, X. Wu, S. P. Diefenbach, B. Kneale, *U. S. Pat. Appl.*, **2009**, 0062492A1. b) T. K. Trefz, M. A. Henderson, M. Y. Wang, S. Collins, J. S. McIndoe, *Organometallics* **2013**, *32*, 3149. c) F. Ghiotto, C. Pateraki, J. Tanskanen, J. R. Severn, N. Lühmann, A. Kusmin, J. Stellbrink, M. Linnolahti, M. Bochmann, *Organometallics* **2013**, *32*, 3354.

[3] a) J. T. Hirvi, M. Bochmann, J. R. Severn, M. Linnolahti, *ChemPhysChem* **2014**, 15, 2732. b) M. S. Kuklin, J. T. Hirvi, M. Bochmann, M. Linnolahti, *Organometallics* **2015**, *34*, 3586.

[4] a) W. Kaminsky, *Macromolecules* **2012**, *45*, 3289. b) H. S. Zijlstra, S. Harder, *Eur. J. Inorg. Chem.* **2015**, 19.

[5] E. Zurek, T. Ziegler, *Prog. Polym. Sci.* **2004**, *29*, 107.

[6] a) E. Zurek, T. Ziegler, *Inorg. Chem.* **2001**, *40*, 3279. b) M. Linnolahti, T. N. P. Luhtanen, T. A. Pakkanen, *Chem. Eur. J.* **2004**, *10*, 5977.

[7] a) J. L. Atwood, D. C. Hrncir, R. D. Priester, R. D. Rogers, *Organometallics* **1983**, *2*, 985. b) M. R. Mason, J. M. Smith, S. G. Bott, A. R. Barron, *J. Am. Chem Soc.* **1993**, *115*, 497. c) C. J. Harlan, M. R. Mason, A. R. Barron, *Organometallics* **1994**, *13*, 2957. d) C. J. Harlan, S. G. Bott, A. R. Barron, *J. Am. Chem. Soc.* **1995**, *117*, 6465. e) M. Watanabi, C. N. McMahon, C. J. Harlan, A. R. Barron, *Organometallics* **2001,** *20,* 460.

[8] a) M. Linnolahti, J. R. Severn, T. A. Pakkanen, *Angew. Chem. Int. Ed.* **2006**, *45*, 3331.; *Angew. Chem.* **2006**, *118*, 3409. b) Z. Boudene, T. De Bruin, H. Toulhoat, P. Raybaud, *Organometallics* **2012**, *31*, 8312. c) Z. Falls, N. Tymińska, E. Zurek, *Macromolecules*, **2014**, *47*, 8556. d) Z. Falls, E. Zurek, J. Autschbach, *Phys.Chem.Chem.Phys.* **2016**, *18*, 24106.

[9] a) L. Negureanu, R. W. Hall, L. G. Butler, L. A. Simeral, *J. Am. Chem. Soc.* **2006**, *128*, 16816. b) M. Linnolahti, J. R. Severn, T. A. Pakkanen *Angew. Chem. Int. Ed.* **2008**, *47*, 9279.; *Angew. Chem.* **2008**, *120*, 9419. c) R. Glaser, X. Sun, *J. Am. Chem. Soc.* **2011**, *133*, 13323. d) M. Linnolahti, A. Laine, T. A. Pakkanen, *Chem. Eur. J.* **2013**, *19*, 7133.

[10] D. W. Imhoff, L. S. Simeral, S. A. Sangokoya, J. H. Peel, *Organometallics* **1998**, *17*, 1941.

[11] a) E. W. Hanson, R. Blom, P. O. Kvernberg *Macromol. Chem. Phys.* **2001**, *202*, 2880. b) D. E. Babushkin, N. V. Semikolenova, V. N. Panchenko, A. P. Sobolev, V. A. Zakharov, E. P. Talsi, *Macromol. Chem. Phys.* **1997**, *198*, 3845. c) K. von Lacroix, B. Heitmann, H. Sinn, *Macromol. Symp.* **1995**, *97*, 137. d) D. E. Babushkin, H.-H. Brintzinger, *J. Am. Chem. Soc.* **2002**, *124*, 12869. e) J. Stellbrink, A. Niu, J. Allgaier D. Richter, B. W. Koenig, R. Hartmann, G. W. Coates, L. J. Fetters, *Macromolecules* **2007**, *40*, 4972.

[12] C. Ehm, G. Antinucci, P. H. M. Budzelaar, V. Busico, *J. Organomet. Chem.* **2014**, *772-773*, 161.

[13] Y. Zhao, D. G. Truhlar, *Theor. Chem. Acc.* **2008**, *120*, 215.

[14] B. G. Willis, K. F. Jensen, *J. Phys. Chem. A* **1998**, *102*, 2613.

[15] a) S. Tobisch, T. Ziegler, *J. Am. Chem. Soc.* **2004**, *126*, 9059. b) C. Ehm, R. Cipullo, P. H. M. Budzelaar, V. Busico, *Dalton Trans.* **2016**, *45*, 6847. c) F. Zaccaria, C. Ehm, P. H. M. Budzelaar, V. Busico, *ACS Catal.*

2017, *7*, 1512. d) F. Zaccaria, R. Cipullo, P. H. M. Budzelaar, V. Busico, C. Ehm, *J. Polym. Sci., Part A: Polym. Chem.* **2017**, *55*, 2807.

[16] a) T. K. Trefz, M. A. Henderson, M. Linnolahti, S. Collins, J. S. McIndoe, *Chem. Eur. J.* **2015**, *21*, 2980. b) H. S. Zijlstra, M. Linnolahti, S. Collins, J. S. McIndoe, *Organometallics* **2017**, *36*, 1803.

[17] D. Cam, E. Albizzati, *Makromol. Chem.* **1990**, *191*, 1641.

[18] A. Schaefer, C. Huber, R. Ahlrichs, *J. Chem. Phys.* **1994,** *100,* 5829.

[19] Gaussian 09, Revision C.01, M. J. Frisch, G. W. Trucks, H. B. Schlegel, G. E. Scuseria, M. A. Robb, J. R. Cheeseman, G. Scalmani, V. Barone, B. Mennucci, G. A. Petersson, H. Nakatsuji, M. Caricato, X. Li, H. P. Hratchian, A. F. Izmaylov, J. Bloino, G. Zheng, J. L. Sonnenberg, M. Hada, M. Ehara, K. Toyota, R. Fukuda, J. Hasegawa, M. Ishida, T. Nakajima, Y. Honda, O. Kitao, H. Nakai, T. Veven, J. A. Montgomery, J. E. Peralta, F. Ogliaro, M. Bearpark, J. J. Heyd, E. Brothers, K. N. Kudin, V. N. Staroverov, T. Keith, R. Kobayashi, J. Normand, K. Raghavachari, A. Rendell, J. C. Burant, S. S. Iyengar, J. Tomasi, M. Cossi, N. Rega, J. M. Millam, M. Klene, J. E. Knox, J. B. Cross, V. Bakken, C. Adamo, J. Jaramillo, R. Gomperts, R. E. Stratmann, O. Yazyev, A. J. Austin, R. Cammi, C. Pomelli, J. W. Ochterski, R. L. Martin, K. Morokuma, V. G. Zakrzewski, G. A. Voth, P. Salvador, J. J. Dannenberg, S. Dapprich, A. D. Daniels, O. Farkas, J. B. Foresman, J. V. Ortiz, J. Cioslowski, D. J. Fox, Gaussian, Inc., Wallingford, CT, **2010**.

Entry for the Table of Contents (Please choose one layout)

Layout 1:

ARTICLE

Structure of methylaluminoxane: Combined quantum chemical and mass spectrometric studies reveal the main structural features of the methylaluminoxane activator in olefin polymerization catalysis

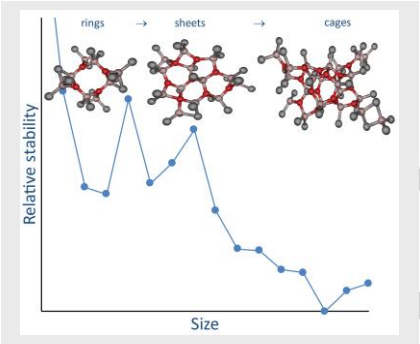

Mikko Linnolahti, Scott Collins*

Page No. – Page No.

Polymerization catalysis